Boiling on a Straight Pin Fin

W. W. Lin and D. J. Lee
Dept. of Chemical Engineering, National Taiwan University, Taipei, Taiwan, 10617 ROC

In this study, Multimode boiling on a straight pin is theoretically investigated. Axial steady-state temperature distributions along the fin are numerically evaluated, as well as their linear stability characteristics. When film and transition boiling coexist on the fin surface, or only the transition boiling covers the entire fin, the operation remains stable only if the fin length is less than some critical value. When transition and nucleate boiling coexist on a fin, or the fin is in the three-mode boiling (film + transition + nucleate boiling), the entry of nucleate boiling at the fin tip stabilizes the boiling process. This study on base heat flow and fin efficiency with the stability criteria also suggests a new fin design methodology.

Introduction

The investigations on fins with a constant heat-transfer coefficient are summarized in several works (Kern and Kraus, 1972; Lienhard, 1987). When boiling occurs on a fin, the heat-transfer coefficient along the fin does not remain constant. Instigated by the pioneering works of Haley and Westwater (1965, 1966) and Lai and Hsu (1967), fin boiling process has received extensive attention. Kraus (1988) reviewed related literature before 1987; Liaw and Yeh (1994a) did the same for literature after 1987. During experiments, the heat-transfer rate might be increased by an order as compared with the case without a fin. Liaw and Yeh (1994b) indicated that the burnout wall superheat shifts from 18.5 to 280 K, thereby broadening the operational temperature range markedly. Consequently, applying boiling on a fin does not serve the conventional purpose of improving heat transfer from a fluid with poor heat-transfer characteristics. On the contrary, it further enhances the high heat-transfer rate that could originally be achieved by boiling and is, therefore, potentially useful in compact heat-exchanger design (Kraus, 1988).

When liquid boils on a fin, the heat-transfer mechanism is much more complicated than the convective ones. For instance, when the fin base temperature is located in the film boiling region, at least three situations might occur on the fin surface: film boiling alone, film followed by transition boiling, and film + transition + nucleate boiling. Obviously, the material's melting point must be higher than the maximum temperature considered here. By assuming a power-law type temperature dependence of the heat-transfer coefficient for each boiling mode, the steady-state temperature distribution along the fin and the base heat flow for various boiling configurations can be found (Unal, 1985; Yeh and Liaw, 1990a; Sen and Trinh, 1986). Fin effectiveness and fin efficiency can then be evaluated from these data and, subsequently, the fin design information is obtained (Unal, 1985; Liaw and Yeh, 1990; Yeh and Liaw, 1990a,b). A prerequisite for using these steady-state solutions in practice is that they are at least stable with regard to infinitesimal perturbations. However, to our knowledge, no previous literature provides comprehensive analysis on their stability characteristics.

Liaw and Yeh (1994a) analyzed stability characteristics for only one boiling mode on the fin. Their results indicate that a fin with only transition boiling on it cannot function properly except with a small fin aspect ratio and/or a quite low thermal conductivity; both conditions are unfavorable to heat-transfer augmentation. The steady-state solutions with only transition boiling on the fin are therefore mostly *unstable* in nature and are of little practical interest. On the other hand, no information regarding the stability characteristics for multimode boiling is available. Therefore, how to design a fin under multimode boiling condition remains unclear.

In this study, we investigate the steady-state solution for boiling on a straight pin fin and the associated stability characteristics. A new concept of fin design methodology is proposed as well.

Basic Equations

A pin fin (of length L and diameter D) with an insulating tip (shown in Figure 1) is selected for detailed analysis since

Correspondence concerning this article should be addressed to D. J. Lee.

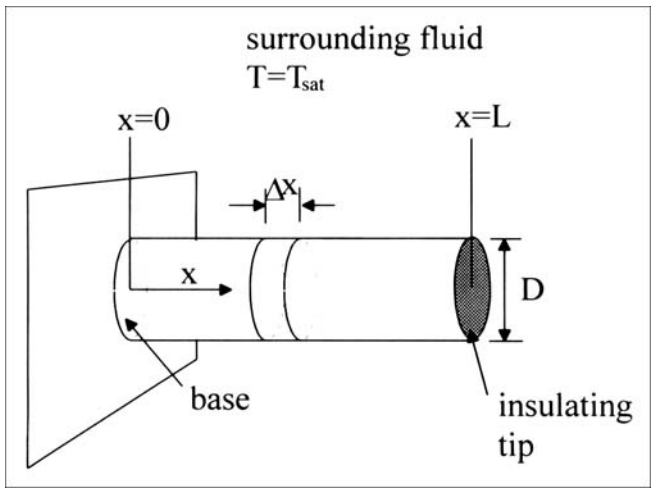

Figure 1. Pin fin.

the basic characteristics are the same for the other one-dimensional straight fins. The origin is set at the fin base and the positive direction is toward the fin tip. The boiling heat-transfer coefficient h_j is assumed here to be a power-law function of wall superheat

$$h_j = a_j(T_j - T_{sat})^{N_j} \tag{1}$$

where T_j is the surface temperature (K), T_{sat} the saturation temperature, a_j the fitting constant, N_j the fitting exponent, and $j = 1$, 2 and 3 denote film, transition, and nucleate boiling, respectively. The power-law type dependence shown in Eq. 1 is widely employed in boiling literature (Lai and Hsu, 1967; Unal, 1985, 1986). More complicated empirical correlation can also be found in previous literature, such as Lee and Lu (1992). However, we note that the basic process characteristics remain unchanged when the more complicated equations are employed.

By assuming a constant thermal conductivity of the fin, the dimensionless governing equation with the heat-transfer coefficient given in Eq. 1 reads (Liaw and Yeh, 1994a)

$$\frac{\partial \Theta_j}{\partial \tau} = \frac{\partial^2 \Theta_j}{\partial X^2} - M_j^2 \Theta_j^{N_j+1}, \tag{2}$$

where

$$\Theta_j = \frac{T_j - T_{sat}}{T_b - T_{sat}}, \quad X = \frac{x}{L}, \quad \tau = \frac{\alpha t}{L^2},$$

$$M_j^2 = \left(\frac{4\alpha_j L^2 (T_b - T_{sat})^{N_j}}{kD} \right), \tag{3}$$

The two boundary conditions at the origin and the insulating tip are

$$\Theta_j(0) = 1, \quad d\Theta_k(1)/dX = 0. \tag{4}$$

Other boundary conditions appear when multimode boiling occurs, including the continuation of temperature and heat flux at the interfaces between different modes.

The index system requires explanation. $i = j = k = 1$, 2 or 3 for the fin covered entirely by film boiling (referred to as the F mode), transition boiling (the T mode), or nucleate boiling (the N mode). $j = 1$ or 2 in Eq. 2 and $i = 1$, $k = 2$ in Eq. 4 when the film and transition boiling coexist on the fin surface (the FT mode). $j = 2$ or 3 in Eq. 2 and $i = 2$, $k = 3$ in Eq. 4 when transition and nucleate boiling coexist on the fin surface. $j = 1$, 2 or 3 in Eq. 2 and $i = 1$, $k = 3$ in Eq. 4 if film, transition and nucleate boiling coexist on the fin surface (the FTN mode). The corresponding steady-state temperature distributions can be found in Unal (1985) and are not repeated here for brevity sake.

Here, the boiling curve data (a complete description of Eq. 1) for saturated isopropanol reported in Unal (1987) are utilized in the following sample calculations (a_1, a_2, $a_3 = 254$, 2.92×10^8, 28 W/m^2·K$^{-N_j-1}$, and N_1, N_2, $N_3 = 0$, -3.18, 2). Notably, the parameters for transition boiling are modified owing to the existence of discontinuity points on the boiling curve constructed by the parameters given in Unal (1987). However, boiling experiments usually do not reveal such discontinuity. Nevertheless, the modified boiling curve exhibits a continuous character.

If N_j equals some certain values, an analytical solution can be found for the temperature distributions along the fin (Unal, 1985). In this work, $N_2 = -3.18$ which was not included in the list makes numerical integration necessary. Since a singularity exists in evaluation of the steady-state solutions, a numerical scheme combining the Romberg integration formula with the Gaussian quadrature is employed here. The relative error for convergence is set at 10^{-6}.

Results

The calculated dimensionless base heat flows Q_b and Θ_t/Θ_{MHF} for $1/\Theta_{MHF} = 1.235$, 0.617, or 0.247 (where the base temperature is located in film, transition, or nucleate boiling region) are plotted against the aspect ratio in Figures 2a and 2b. Notably, subscripts t and MHF denote tip and minimum heat flux points, respectively. Clearly, Q_b increases and Θ_t/Θ_{MHF} decreases monotonously with an increasing aspect ratio when $1/\Theta_{MHF}$ is low (0.247). No hysteresis occurs. However, when the base temperature increases ($1/\Theta_{MHF} = 1.235$ or 0.617), an obvious S-shaped relationship is observed in which some range of L/D three steady-state solutions exist.

Consider the case with $1/\Theta_{MHF} = 1.235$ as an example. The tip temperature in Figure 2b demonstrates that the upper steady-state solution is in F mode (point A), the middle in FT mode (point B), and the lower one FTN mode (point C). As discussed later in detail, point B is an unstable steady state and is inaccessible in practice.

Q_b approaches a plateau value when the fin aspect ratio further increases. Therefore, an extremely long fin incurs no benefit since the temperature for most fin surfaces is too close to the surrounding temperature. If the fin is made of copper with a diameter of 1 or 3 mm, the plateau heat flux can reach as high as 4.64×10^6 or 1.55×10^6 W/m^2 when $1/\Theta_{MHF} = 1.235$. Those values are 14 or 4.7 times that of the critical heat flux (CHF, $= 3.28 \times 10^5$ W/m^2 in this boiling system), i.e., significantly higher than the conventional convective fins. This finding suggests the potential of applying boiling on fin process to high heat flux systems.

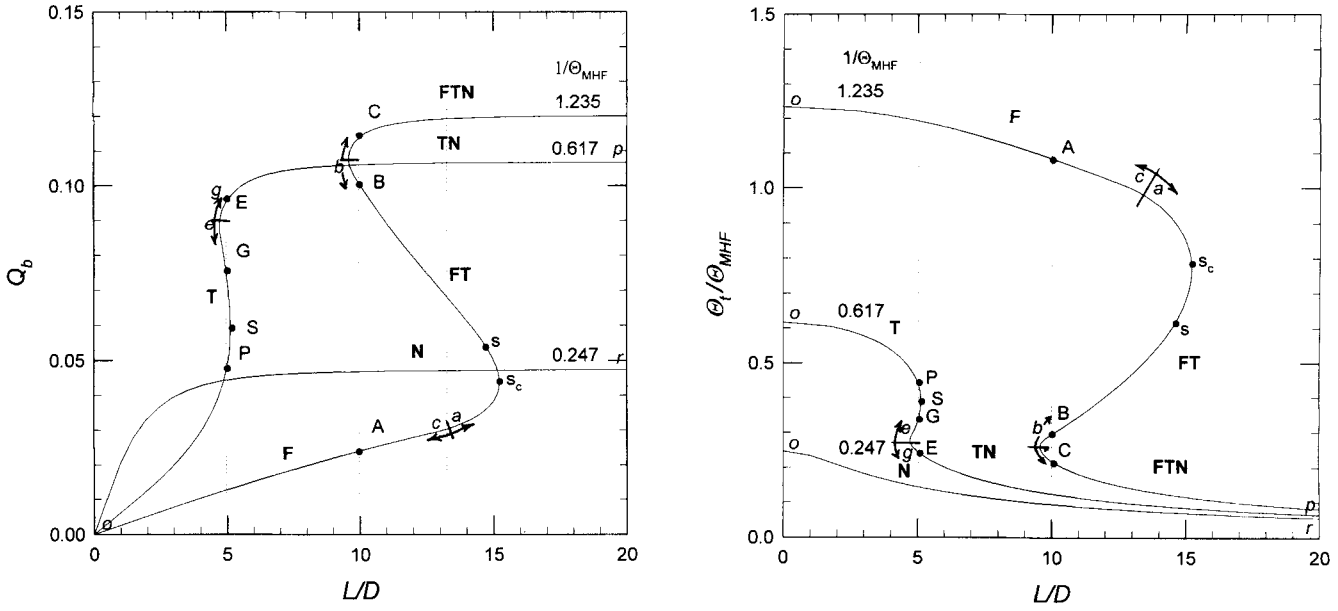

Figure 2. (a) Q_b vs. L/D; (b) Θ_t/Θ_{MHF} vs. L/D.

With the base heat flow data calculated above, the efficiency (η_f), i.e., the ratio between the calculated base heat flow to the total heat flow transferred from a fin with the entire surface under the base temperature, can be obtained (Lienhard, 1987). Figure 3 summarizes those results. In F or N mode boiling, fin efficiency is less than unity, which corresponds to the fact that owing to the decrease in temperature along the fin, the heat-transfer rate would reduce correspondingly (N_1 and N_3 are both ≥ 0). In all other cases, fin efficiency is generally well above unity except for a short portion of FT mode or those with a very long fin. Such a circumstance arises from the incorporation of transition boiling whose heat-transfer coefficient increases with decreasing wall superheat ($N_2 < 0$). This feature makes the incorporation of transition boiling mode attractive, although it is essentially unstable in nature.

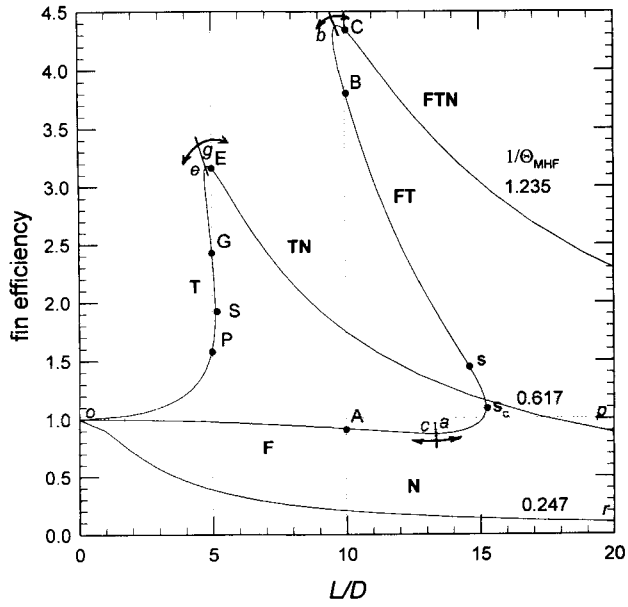

Figure 3. Fin efficiency vs. fin aspect ratio.

S-shaped curve appears when L/D has exceeded some value in which the efficiency becomes a triple-valued function. This function corresponds to the three steady-state region shown in Figures 2 and 3. Clearly in multimode boiling, fin efficiency not only increases rapidly with an increasing aspect ratio, but also attains a maximum when nucleate boiling just enters at the fin tip. For the present example, the maximum η_f value is 3.2 or 4.3 when $1/\Theta_{MHF} = 0.617$ or 1.235. After passing the maximum, the efficiency decreases as aspect ratio further increases, and eventually drops to zero when the aspect ratio becomes infinite.

Linear Stability Analysis

In this section, we perform linear stability analysis on the steady-state solution of Eq. 2. If an infinitesimal temperature perturbation $\overline{\Theta}_j(X, \tau)$ is imposed onto the steady-state solution, i.e., $\Theta_j(X, \tau) = \Theta_j^s(X) + \overline{\Theta}_j(X, \tau)$ where Θ_j^s is the steady-state temperature distribution and is a function of X only, Eq. 2 can be linearized and the result reads as follows

$$\frac{\partial \overline{\Theta}_j}{\partial \tau} = \frac{\partial^2 \overline{\Theta}_j}{\partial X^2} - M_j^2 (N_j + 1)(\Theta_j^s)^{N_j} \overline{\Theta}_j. \tag{5}$$

The two boundary conditions in Eq. 4 become

$$\overline{\Theta}_i(0) = 0; \quad d\overline{\Theta}_k(1)/dX = 0. \tag{6}$$

Equation 5 with Eq. 6 form an eigenvalue problem. The sign of the maximum eigenvalue determines the stability of the steady state.

One-mode boiling

Previously, Liaw and Yeh (1994a) performed linear stability analysis for one-mode boiling, indicating that the maximum eigenvalue is

$$\lambda_{\max} = -M_j^2(N_j+1)\Theta_t^{N_j} - \frac{\pi^2}{4}, \tag{7}$$

where $j = 1$, 2, or 3 for N, T, or F mode, respectively. Figure 4 shows some $\lambda_{\max}$s. All results for F (curve oc) or N mode (curve or) are negative, implying a stable one-mode boiling process. In T mode, $\lambda_{\max}^T$ is negative along curve oS, and becomes a two-value function when L/D has exceeded some critical value. The upper solution follows curve Se. Moreover, Figures 2 and 3 illustrate the S point separating stable and unstable T mode. The point P (point G) in Figures 2 to 3 is thereby stable (unstable).

Two-mode boiling

Consider a fin under FT mode. The solutions $\overline{\Theta}_1 = \Phi_1(X)\exp(\lambda\tau)$ and $\overline{\Theta}_2 = \Phi_2(X)\exp(\lambda\tau)$ for the linearized governing equations (Eq. 5 with $j = 1$ or 2) are searched for. The problem is then reduced to the following eigenvalue problem

$$\frac{d^2\Phi_1}{dX^2} + \Gamma_1(X)\Phi_1 = 0, \quad 0 < X < X_f, \tag{8a}$$

$$\frac{d^2\Phi_2}{dX^2} + \Gamma_2(X)\Phi_2 = 0, \quad X_f < X < 1, \tag{8b}$$

where X_f is the dimensionless position separating film and transition boiling modes

$$\Gamma_1(X) = -\lambda - M_1^2(N_1+1)(\Theta_1^S)^{N_1}, \tag{9a}$$

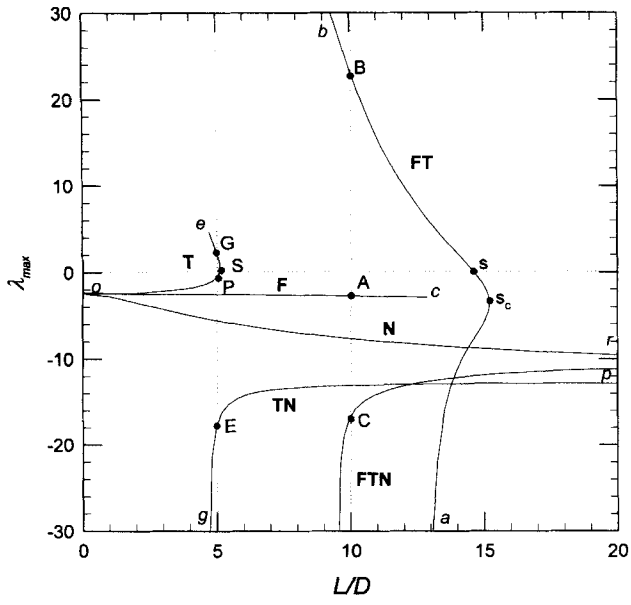

Figure 4. Maximum eigenvalue vs. fin aspect ratio.

$$\Gamma_2(X) = -\lambda - M_2^2(N_2+1)(\Theta_2^S)^{N_2}, \tag{9b}$$

The boundary conditions read as

$$\Phi_1(0) = 0, \quad \Phi_1(X_f) = \Phi_2(X_f), \quad \frac{d\Phi_1(X_f)}{dX} = \frac{d\Phi_2(X_f)}{dX}, \quad \frac{d\Phi_2(1)}{dX} = 0. \tag{10}$$

From Eqs. 8a and 8b, the following equation can be obtained

$$-\int_0^{X_f}(\Phi_1')^2dX - \int_{X_f}^1(\Phi_2')dX + \int_0^{X_f}\Gamma_1(\Phi_1)^2dX + \int_{X_f}^1\Gamma_2(\Phi_2)^2dX = 0, \tag{11}$$

where Φ_j' denotes $d\Phi_j/dX$. The condition for the existence of nonzero solution for Eqs. 8a and 8b is derived in the Appendix and the following inequalities hold

$$\int_0^{X_f}(\Phi_1')^2dX \geq \frac{\pi^2}{4X_f^2}\int_0^{X_f}\Phi_1^2dX, \tag{12a}$$

$$\int_{X_f}^1(\Phi_2')^2dX \geq \frac{\pi^2}{4(1-X_f)^2}\int_{X_f}^1\Phi_2^2dX. \tag{12b}$$

Therefore, from Eqs. 11, 12a and 12b, the following inequality is obtained

$$\left(-\frac{\pi^2}{4X_f^2} + \sup\Gamma_1\right)\int_0^{X_f}(\Phi_1)^2dX + \left(-\frac{\pi^2}{4(1-X_f)} + \sup\Gamma_2\right)\int_{X_f}^1(\Phi_2)^2dX \geq 0. \tag{13}$$

The maximum eigenvalue can then be obtained by setting Eq. 13 equal to zero.

Since the integrals in Eq. 13 are all definitely positive, with some logical arguments, the maximum eigenvalue can be found as

$$\lambda_{\max}^{FT} = \frac{-1}{1+\omega}\left\{\frac{\pi^2}{4X_f^2} + \frac{\pi^2\omega}{4(1-X_f)^2} + M_1^2(N_1+1)\Theta_{MHF}^{N_1} + M_2^2(N_2+1)\Theta_t^{N_2}\omega\right\} = \frac{1}{1+\omega}(\lambda_{\max}^F + \omega\lambda_{\max}^T), \tag{14}$$

where

$$\omega = \frac{\int_{X_f}^{1} \Phi_2^2 dX}{\int_0^{X_f} \Phi_1^2 dX}, \tag{15}$$

and $\lambda_{\max}^{F}$ and $\lambda_{\max}^{T}$ are evaluated in $[0, X_f]$ and $[X_f, 1]$, respectively.

Clearly $\lambda_{\max}^{FT}$ in Eq. 14 is a weighted average for $\lambda_{\max}^{F}$ and $\lambda_{\max}^{T}$ with parameter ω ranging from zero to infinity. When $\omega \to 0$, Eq. 14 becomes Eq. 7 with $j = 1$, which is for F mode. When $\omega \to \infty$, Eq. 14 becomes Eq. 7 with $j = 2$, which is for T mode.

In a similar manner, the stability criteria for a fin under TN mode is

$$\lambda_{\max}^{TN} = \frac{-1}{1+\beta}\left\{\frac{\pi^2}{4X_d^2} + \frac{\pi^2\beta}{4(1-X_d)^2} + M_2^2(N_2+1)\Theta_{CHF}^{N_2} + M_3^2(N_3+1)\Theta_t^{N_3}\beta\right\} = \frac{1}{1+\beta}(\lambda_{\max}^{T} + \beta\lambda_{\max}^{N}), \tag{16}$$

$$\beta = \frac{\int_{X_d}^{1} \Phi_3^2 dX}{\int_0^{X_d} \Phi_2^2 dX}, \tag{17}$$

and $\lambda_{\max}^{T}$ and $\lambda_{\max}^{N}$ are evaluated in $[0, X_d]$ and $[X_d, 1]$, respectively. Notably, X_d is the dimensionless position separating transition and nucleate boiling modes.

As under FT mode, $\lambda_{\max}^{TN}$ is also a weighted average for $\lambda_{\max}^{T}$ and $\lambda_{\max}^{N}$ with parameter β ranging from zero to infinity. When $\beta \to 0$, Eq. 16 reduces to Eq. 7 with $j = 2$, which is for T mode. As $\beta \to \infty$, Eq. 16 becomes Eq. 7 with $j = 1$, the N mode.

To evaluate ω or β, information regarding the Φs is required. Function Φ controls the manner (shape) in which the steady-state temperature distribution is perturbed, which is unknown in practice. Many possibilities are available for the function Φ (if only they satisfy BC Eq. 10), thereby making it impractical to examine all of the cases. This is also the major difficulty encountered in analyzing the stability characteristics for axial distributed systems with multiple steady-state coexistence. However, if the output for maximum eigenvalue is insensitive to the functional forms for the Φs, then all the trial functions can be used.

The following six functions satisfying Eq. 10 are tested

$$\Phi = X^2 - 2X, \quad \Phi = X^3 - 3X, \quad \Phi = X^5 - 5X, \quad \Phi = X^7 - 7X, \quad \Phi = \frac{1}{3}X^3 - \frac{1}{2}X^2, \quad \Phi = \sin\left(\frac{\pi}{2}X\right). \tag{18a–f}$$

Using Eqs. 18a to 18f yields an almost immaterial $\lambda_{\max}^{FT}$ and $\lambda_{\max}^{TN}$, thereby suggesting that each of the Eqs. 18a–18f can be used. Figure 4 presents the numerical results.

In TN mode (curve gp), all $\lambda_{\max}^{TN}$s are negative, indicating a stable boiling process at point E in Figures 2 to 3. Compared with the T mode boiling at point G, the appearance of the nucleate boiling at tip stabilizes the boiling process.

In FT mode (curve ab), the maximum eigenvalue can be negative (curve as) or positive (curve sb) depending on the tip temperature. Therefore, the FT mode at point B in Figures 2 to 3 is unstable.

To obtain further insight, the values of $\lambda_{\max}^{T}$, $\lambda_{\max}^{N}$, and β for $\lambda_{\max}^{TN}$, and the value of $\lambda_{\max}^{T}$, $\lambda_{\max}^{F}$ and ω for $\lambda_{\max}^{FT}$ are shown in Figures 5a and 5b, respectively. For the TN mode, when nucleate boiling just enters at tip (point g), $X_d \to 1$ and

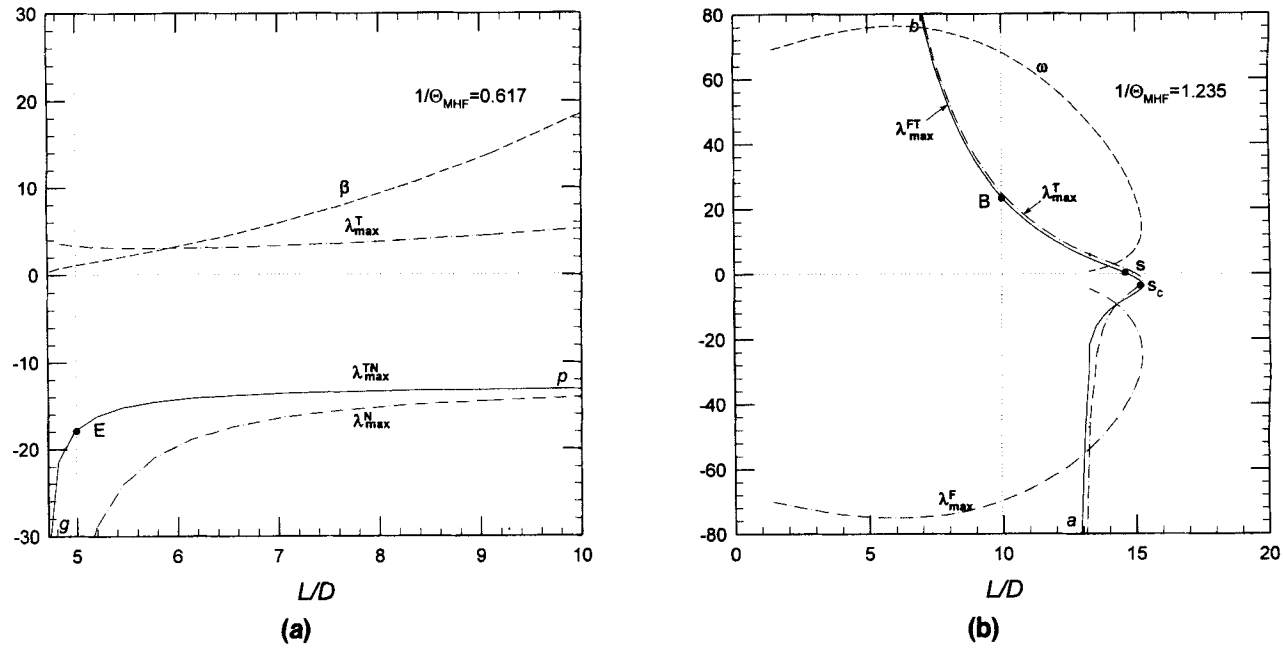

Figure 5. (a) $\lambda_{\max}^{N}$, $\lambda_{\max}^{T}$, β and $\lambda_{\max}^{TN}$ vs. L/D; (b) $\lambda_{\max}^{F}$, $\lambda_{\max}^{T}$, ω and $\lambda_{\max}^{FT}$ vs. L/D.

$\beta \to 0$. The corresponding tip temperature is close to CHF point which makes $\lambda^N_{\max}$ a very negative value and, thereby, a negative $\lambda^{TN}_{\max}$. When fin aspect ratio grows, the tip temperature (and also the absolute value of $\lambda^N_{\max}$) decays and $\lambda^T_{\max}$ increases. Nevertheless, the growing β compensates the unstable component and keeps the maximum eigenvalue negative, as shown in Figure 5a.

In *FT* mode, multiple solutions are possible. When transition boiling just enters at fin tip (point a), both $\lambda^T_{\max}$ and $\lambda^F_{\max}$ are negative. The subsequent $\lambda^{FT}_{\max}$ is thereby negative, as demonstrated in Figure 5b. When tip temperature is further decreased, the magnitudes of the decrease of $\lambda^F_{\max}$ and increase of ω are small when compared with the growth of $\lambda^T_{\max}$, which results in a positive $\lambda^{FT}_{\max}$ (curve sb). Therefore, point B in Figures 2 to 3 is an unstable *FT* mode.

From the linear stability analysis, the middle regions for the S-shaped curves in *T* mode boiling are all identified as unstable, i.e., the S point almost coincides with the critical points of the S-shaped curves (Figure 4). However, in *FT* mode, a small deviation occurs between point s and the critical point s_c (Figure 5b). Numerical investigation by perturbing the steady-state solution on the curve $s-s_c$ with a finite amplitude reveals that the steady-state solutions are actually unstable. The discrepancy might be due to the inherent limit for the employment of linear stability analysis onto such a highly nonlinear process; otherwise, the functional forms of Φs examined in this work are not absolutely adequate. This problem remains unresolved until the present stage. Nevertheless, owing to a relatively small *FT* region with such a discrepancy, it would not influence the basic stability characteristics and would also not influence the subsequent discussions and conclusion.

Three-mode boiling

For a fin under *FTN* mode, the solutions of the following forms are searched for: $\overline{\Theta}_1 = \Phi_1(X)\exp(\lambda\tau)$, $\overline{\Theta}_2 = \Phi_2(X)\exp(\lambda\tau)$ and $\overline{\Theta}_3 = \Phi_3(X)\exp(\lambda\tau)$. With the inequalities given in the Appendix, the stability criteria for a fin with three-mode boiling can be derived similarly as that for two-mode boiling as follows

$$\lambda^{FTN}_{\max} = \frac{-1}{1+\gamma+\delta}\left\{\frac{\pi^2}{4X_f^2} + \frac{\pi^2\gamma}{4(X_d - X_f)^2} + \frac{\pi^2\delta}{4(1-X_d)^2} + M_1^2(N_1+1)\Theta^{N_1}_{MHF} + M_2^2(N_2+1)\Theta^{N_1}_{CHF}\gamma + M_3^2(N_3+1)\Theta_t^{N_3}\delta\right\}$$

$$= \frac{1}{1+\gamma+\delta}(\lambda^F_{\max} + \gamma\lambda^T_{max} + \delta\lambda^N_{\max}), \quad (19)$$

where

$$\gamma = \frac{\int_{X_f}^{X_d}\Phi_2^2 dX}{\int_0^{X_f}\Phi_1^2 dX}, \quad \delta = \frac{\int_{X_d}^{1}\Phi_3^2 dX}{\int_0^{X_f}\Phi_1^2 dX}, \quad (20a,b)$$

where $\lambda^F_{\max}$, $\lambda^T_{\max}$ and $\lambda^N_{\max}$ are evaluated in the domain $[0, X_f]$, $[X_f, X_d]$ and $[X_d, 1]$, respectively. The $\lambda^{FTN}_{\max}$ is therefore a weighted average for $\lambda^F_{\max}$, $\lambda^T_{\max}$, and $\lambda^N_{\max}$ with parameters γ and δ ranging from zero to infinity. When both γ and δ approach zero, Eq. 19 becomes Eq. 7 with $j = 1$, which is for *F* mode. When γ approaches infinity with a finite δ, Eq. 19 becomes Eq. 7 with $j = 2$, which is for *T* mode. When δ approaches infinity with a finite γ, Eq. 19 becomes Eq. 7 with $j = 3$, which is for *N* mode. When δ approaches zero, Eq. 19 becomes Eq. 14, the *FT* mode. When γ and δ both approach infinity, Eq. 19 becomes Eq. 16, i.e., the *TN* mode.

Using Eqs. 18a to 18f to evaluate of $\lambda^{FTN}_{\max}$ yields nearly identical results as well. Figure 4 summarizes those results. Since those values are all negative, *FTN* is a stable boiling mode (point C in Figures 2 to 3), which corresponds to the experimental findings by Haley and Westwater (1965). When compared with the *FT* mode, the appearance of the nucleate boiling at fin tip stabilizes the boiling process. Such a result is similar to that for *T* and *TN* mode boiling.

The output from the stability analysis appears to be obvious, owing to the fact that many other engineering systems exhibiting multiple steady states would commonly have the middle one unstable (such as the catalytic, exothermic reactions in catalyst pellet). This is also the case for a fin covered entirely by one-mode boiling (that is, if the small portion for *stable* transition boiling regime is neglected), as suggested by Liaw and Yeh (1994a). Notably, in those systems, only one steady-state distribution can be selected at one time. Therefore, the middle, unstable steady state would never appear in practice. However, the multimode boiling process examined in this work can have several steady states *coexisting* in the system. That is, an unstable steady state (transition boiling) cannot only steadily exist with the existence of other stable steady state(s), but also provide better heat-transfer performance than the single steady state. The stability characteristics for such a system are not well understood, and therefore, are the primary concern of this work.

Conceptual Methodology of Fin Design

A fin design with boiling should consider its stability characteristics. Although Eq. 1 is a highly uncertain assumption regarding the boiling process, a conceptual design methodology can still be proposed on the basis of the steady-state calculations and the linear stability results obtained in previous sections. Engineering design should be based on more accurate experimental data. However, a similar procedure can be employed as reported here.

Figure 6 plots Q_b against a dimensionless base temperature with a copper fin with $D = 1$ mm. This figure also includes the constant fin efficiency and the constant aspect ratio curves. The unstable region is marked by a dot-dashed envelope which is open in the direction of higher base temperature and covers most regions of a high efficiency. No fin can function properly in the unstable region and, therefore, should be avoided in design.

The maximum efficiency occurs when nucleate boiling just enters at tip in multimode boiling, as indicated in Figure 3. The accumulation of the points with maximum efficiency for various fin aspects ratio forms the bold solid curve in Figure 6 ($\eta_{\max}$). Above this curve are the regions of stable *FT* or *FTN* mode, just below which are the unstable *FT* or stable/unstable *T* mode. The point of highest efficiency oc-

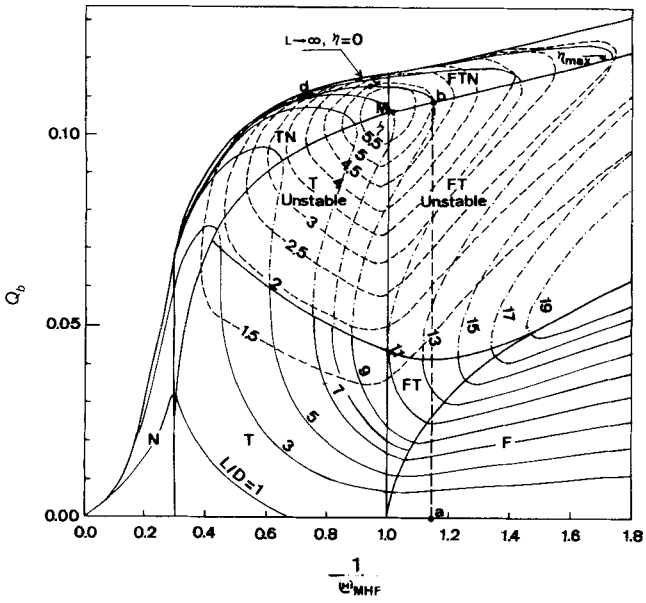

Figure 6. Conceptual design for a fin under boiling.
Copper fin with $D = 1$ mm.

curs at the M-point, where an extremely small region of film boiling exists at fin base with an infinitesimal region of nucleate boiling at fin tip. The conceptually best fin is therefore operated at point M. Nevertheless, owing to the consideration that any small base temperature perturbation might push the nucleate boiling out of the fin and induce instability, a proper length of nucleate boiling section should be allowed to exist in design for tolerating the maximum process perturbation.

For instance, consider a fin design example with a given dimensionless base temperature $1/\Theta_{MHF} = 0.95$ with a maximum relative variation of 0.2. First, locate the maximum base temperature on the abscissa (point a) $(0.95 + 0.2)$, and then find the corresponding point on the maximum efficiency curve (point b). The dimensionless fin length can then be read out as 9.0 from Figure 6. The design point is thereby the intercept between the L/D curve and the $1/\Theta_{MHF} = 0.95$ line (point c). Therefore, for a dimensionless base temperature ranging from 0.75 to 1.15, the dimensionless base heat flow is approximately 0.11 to 0.13 with a fin efficiency of 5.0 to 2.5. Notably, a rather minor change in base heat flow occurs as compared with that in the fin efficiency. That is, such a fin can transfer a near-constant heat flow over a wide range of base temperature variation.

Conclusion

In this study, we have theoretically investigated boiling on a straight pin fin. Steady-state solutions are numerically evaluated and linear stability analysis is performed. For one-mode boiling, the fin is unstable only when the fin base temperature is in transition boiling region; in addition, the fin parameter has exceeded some critical value. For two-mode boiling on a fin, two possibilities occur: film boiling followed by transition boiling or transition boiling followed by nucleate boiling. In the former case, the boiling becomes unstable when the fin parameter exceeds some critical value. For the latter case, the entry of nucleate boiling at fin tip stabilizes the boiling process. For three-mode boiling (film + transition + nucleate boiling), the entry of nucleate boiling at fin tip stabilizes the boiling process. The study on base heat flow and fin efficiency with the stability criteria suggests that the "best" fin should be designed with its tip temperature slightly lower than the critical heat flux (*CHF*) temperature, with a tolerance allowing the base temperature perturbation.

Acknowledgments

The authors would like to thank the National Science Council, R.O.C., for financial support of this work.

Notation

T_b = fin base temperature, K
α = thermal diffusivity, $m^2 s^{-1}$
λ = eigenvalue
λ_{max} = maximum eigenvalue
$\lambda^F_{max}, \lambda^N_{max}$ = maximum eigenvalue for film and nucleate boiling, respectively
λ^T_{max} = maximum eigenvalue for transition boiling
λ^{FT}_{max} = maximum eigenvalue for film boiling followed by transition boiling
λ^{TN}_{max} = maximum eigenvalue for transition boiling followed by nucleate boiling
λ^{FTN}_{max} = maximum eigenvalue for *FTN* boiling
Θ_t = dimensionless tip temperature
Θ_{CHF} = dimensionless temperature where $X = X_d$
Θ_{MHF} = dimensionless temperature where $X = X_f$

Literature Cited

Denn, M. M., *Stability of Reaction and Transport Processes*, Prentice-Hall, Englewood Cliffs, NJ (1985).
Haley, K. W., and J. W. Westwater, "Boiling Heat Transfer from a Single Fin to a Boiling Liquid," *Chem. Eng. Sci.*, **29**, 711 (1965).
Haley, K. W., and J. W. Westwater, "Boiling Heat Transfer from Single Fins," *Proc. Int. Heat Transf. Conf.*, Vol. III, p. 245 (1966).
Kern, D. Q., and A. D. Kraus, *Extended Surface Heat Transfer*, McGraw Hill, New York (1972).
Kraus, A. D., "Sixty-five Years of Extended Surface Technology," *Appl. Mech. Rev.*, **41**, 321 (1988).
Lai, F. S., and Y. Y. Hsu, "Temperature Distribution in a Fin Partially Cooled by Nucleate Boiling," *AIChE J.*, **13**, 817 (1967).
Lee, D. J., and S. M. Lu, "Two Mode Boiling on a Horizontal Heating Wire," *AIChE J.*, **38**, 1115 (1992).
Liaw, S. P., and R. H. Yeh, "Analysis of Pool Boiling Heat Transfer on a Single Cylindrical Fin," *J. Chin. Soc. Mech. Eng.*, **11**, 448 (1990).
Liaw, S. P., and R. H. Yeh, "Fins with Temperature Dependent Surface Heat Flux—I. Single Heat Transfer Model," *Int. J. Heat Mass Transf.*, **37**, 1509 (1994a).
Liaw, S. P., and R. H. Yeh, "Fins with Temperature Dependent Surface Heat Flux—II. Multi-boiling Heat Transfer," *Int. J. Heat Mass Transf.*, **37**, 1515 (1994b).
Lienhard, J. H., *A Heat Transfer Textbook*, 2nd ed., Prentice-Hall, Englewood Cliffs, NJ (1987).
Sen, A. K., and S. Trinh, "An Exact Solution for the Rate of Heat Transfer From a Rectangular Fin Governed by Power Law-Type Temperature Dependence," *J. Heat Transf., Trans. ASME*, **108**, 457 (1986).
Unal, H. C., "Determination of the Temperature Distribution in an Extended Surface with a Non-uniform Heat Transfer Coefficient," *Int. J. Heat Mass Transf.*, **28**, 2279 (1985).
Unal, H. C., "A Simple Method of Dimensioning Straight Fins for Nucleate Pool Boiling," *Int. J. Heat Mass Transf.*, **29**, 640 (1986).
Unal, H. C., "An Analytic Study of Boiling Heat Transfer from a Fin," *Int. J. Heat Mass Transfer*, **30**, 341 (1987).
Yeh, R. H., and S. P. Liaw, "An Exact Solution for Thermal Characteristics of Fins with Power-law Heat Transfer Coefficient," *Int. Comm. Heat Mass Transfer*, **17**, 317 (1990a).
Yeh, R. H., and S. P. Liaw, "Theoretical Study of a Fin Subject to Various Types of Heat Transfer," *Tatung J.*, **20**, 59 (1990b).

Appendix: Proof for the Inequality Required to Derive Eqs. 12a and 12b

We shall prove the following inequality: let $u(z)$ be a bounded differentiable function in a domain $[a, b]$, then

$$\int_a^b \left(\frac{du}{dz}\right)^2 dz \geq \frac{\pi^2}{4(b-a)^2}\int_a^b u^2 dz. \tag{A1}$$

Proof

The proof follows a similar logic as that in Denn (1985). Let function $h(z)$ be any differentiable function in $[a, b]$, then

$$\int_a^b \left(\frac{du}{dz} + \frac{dh}{dz}hu\right)^2 dz \geq 0. \tag{A2}$$

Equation A2 can be expanded and integrated by parts to yield

$$\int_a^b u^2\left(h^2\left(\frac{dh}{dz}\right)^2 - \frac{d(hh')}{dz}\right)dz + \int_a^b \left(\frac{du}{dz}\right)^2 dz + h(b)h'(b)u^2(b) - h(a)h'(a)u^2(a) \geq 0. \tag{A3}$$

Let $y = h'h$, and let $h'(a) = 0$, $h(b) = 0$. Equation A3 can be rearranged as

$$\int_a^b u^2(y^2 - y')dz + \int_a^b \left(\frac{du}{dz}\right)^2 dz \geq 0. \tag{A4}$$

Finally, take $y(z)$ as the solution of the following equation

$$y' - y^2 = C^2, \tag{A5}$$

where C is a constant and $y(z)$ is finite within $a < z < b$, then

$$y(z) = C\tan C(z-a), \tag{A6}$$

with $C \leq \pi/[2(b-a)]$. The most conservative condition is Eq. A1, which completes the proof.

Manuscript received Nov. 13, 1995, and revision received Mar. 25, 1996.